

# **A Non-Metal Emission Detector for HPLC**

Dependent Proposal  
Submitted in partial fulfillment of the degree of  
Doctor of Philosophy

By  
Heather L. Peters

To  
Advisory Committee  
Department of Chemistry  
Wake Forest University

April 19, 2004

## TABLE OF CONTENTS

Introduction . . . . .	1
Instrumentation . . . . .	1
HPLC-ICP System Constraints . . . . .	13
Carbon Determination . . . . .	16
Conclusion . . . . .	19

Appendix A: See pdf link on website.

An Inductively Coupled Plasma Carbon Emission Detector for Aqueous Carbohydrate Separations by Liquid Chromatography

Appendix B

A Multi-Analyte Calibration Curve for High Performance Liquid Chromatography with an Inductively Coupled Plasma Carbon Emission Detector

References

## INTRODUCTION

The present research focuses on three projects designed to provide a universal detection method for compounds that lack chromophores and do not exhibit native fluorescence. Generally these compounds would be derivatized for UV absorption detection or determined using refractive index detection, which has poor sensitivity. An inductively coupled plasma atomic emission spectrometer (ICP-AES) is used as an element specific detector following separation by high performance liquid chromatography (HPLC). After the HPLC separates the compounds in solution, the ICP-AES desolvates, vaporizes, and atomizes the molecules then excites or ionizes the atoms. One or more atomic or ionic emission lines are monitored from the emitted spectra to use as the basis in determining the quantity of the compound present in the sample. The first two projects monitor carbon emission from carbohydrates (Appendix A) and amino acids (Appendix B), respectively. The third project will monitor phosphorus in phospholipids.

## INSTRUMENTATION

A liquid chromatography system is composed of a solvent delivery system, sample introduction system, column, detector, and output system. Figure 1 is a diagram of the HPLC system used for these projects. The system's solvent delivery system has four solvent bottles, a four-channel vacuum degasser, and a quaternary pump (with a multi-channel gradient valve) capable of flow rates from 1  $\mu\text{L}/\text{min}$  to 10  $\text{mL}/\text{min}$  up to 400 bar.<sup>1</sup> The solvent delivery system is diagramed in Figure 2.

**Figure 1. Hewlett-Packard Series 1100 HPLC.**

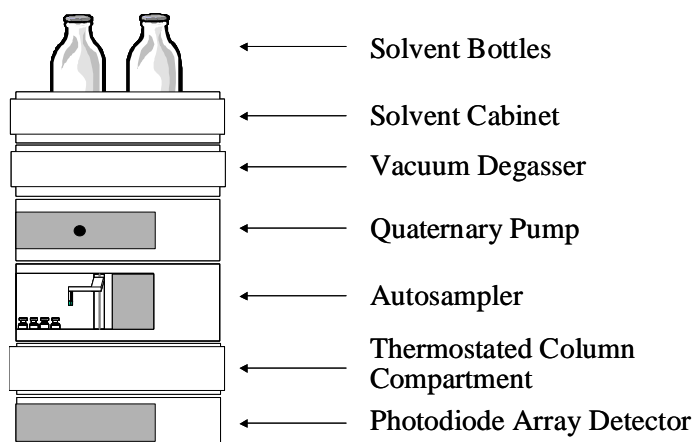
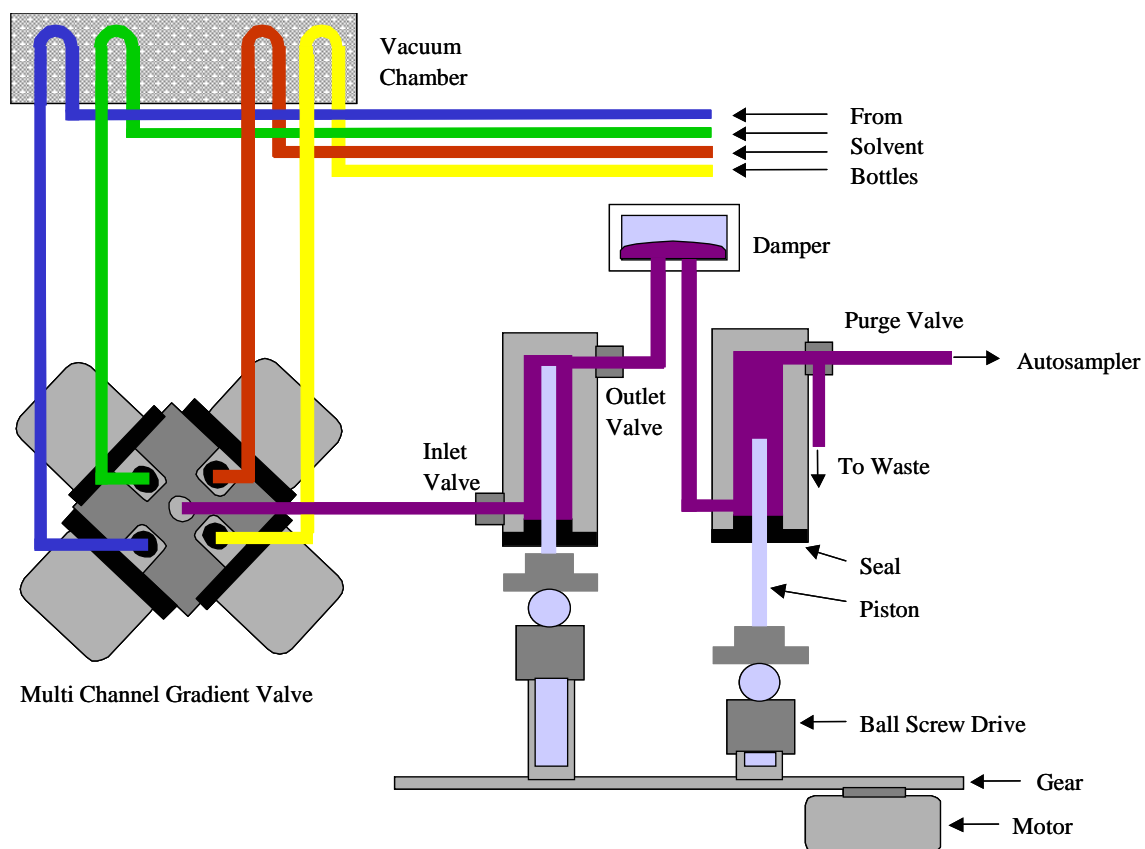
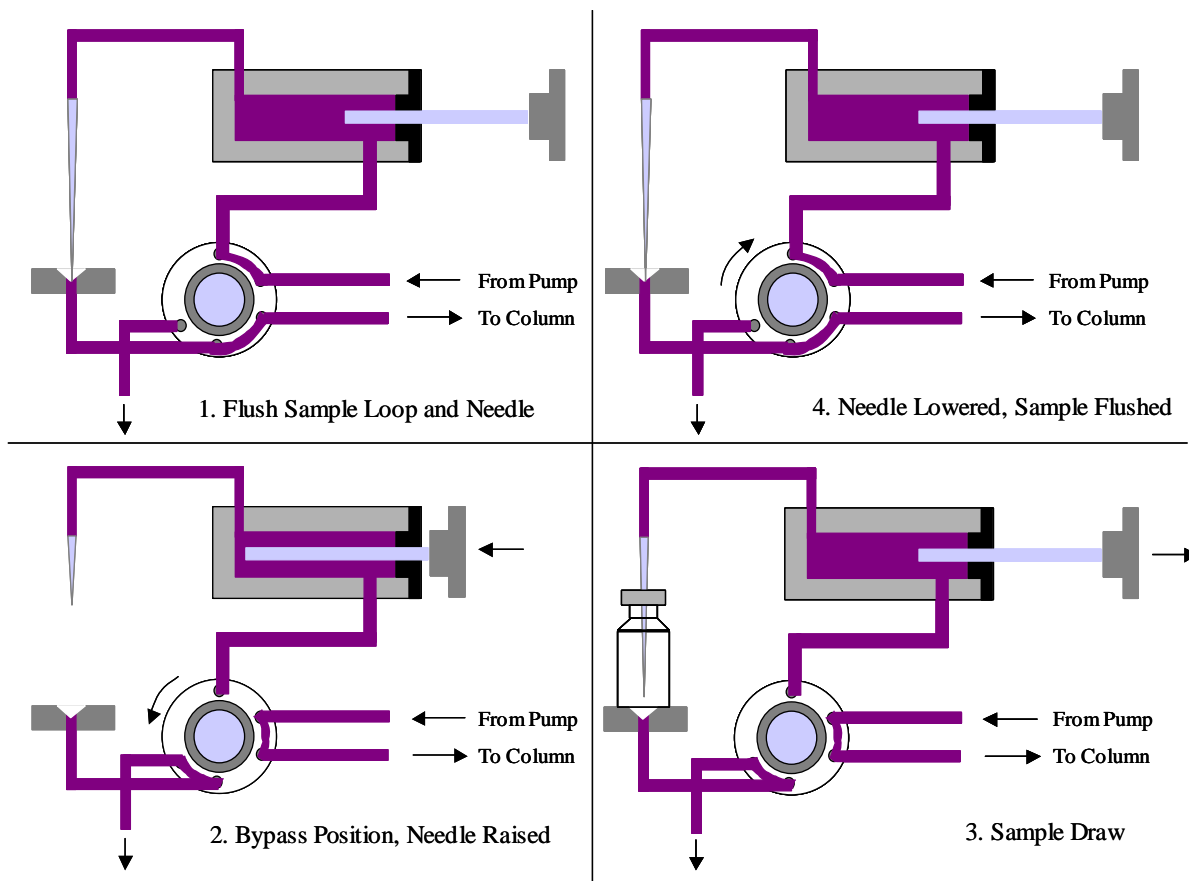


Figure 2. Solvent Delivery System.



The sample introduction system is an autosampler capable of injection volumes of 0.1 – 100  $\mu\text{L}$  with a six-port injection valve, of which five ports are used.<sup>2</sup> The sampling sequence is diagramed in Figure 3. Before the start of the injection cycle and during analysis, the injection valve flows the mobile phase through the autosampler metering device, sample loop, and needle, performing a flush of the system. When sampling begins, the valve switches to the bypass position causing the mobile phase to flow directly from the pump to the column. The metering valve piston goes forward, the needle is raised, the sample vial positioned, the needle inserted, and then the metering unit draws the sample into the sample loop. The needle is then raised, the vial replaced in the sample tray, and the needle lowered into the needle seat. Finally, the injection valve switches into the flush position, flowing the sample onto the column.

**Figure 3. Injection Sequence.**

The thermostated column compartment is capable of controlling temperatures isothermally between 10 degrees below ambient to 80°C.<sup>3</sup> The photodiode array (PDA) detector is composed of a deuterium lamp as the UV light source, emitting over the 190-nm to 800-nm wavelength range and a tungsten lamp as the visible light source, emitting over the wavelength range 470-950 nm.<sup>4</sup> The slit width is programmable from 1 – 16 nm to optimize sensitivity, linearity, and spectral resolution. A standard flow cell with a 10 mm path length and 13 µL volume is employed. A Hewlett-Packard ChemStation is used to control the instrument and manage the output.

The ICP-AES used for these projects is a Leeman Labs Direct Reading Echelle. The ICP-AES is composed of a sample introduction system, plasma, monochromator, detector, and output system. See Figure 4. The eluent from the HPLC flows into the ICP-AES through a 1-m length of 0.178-mm-i.d. x 1.59-mm-o.d. polyetheretherketone (PEEK) tubing where it is converted to an aerosol through a process called pneumatic nebulization. The tube's inner diameter is matched to that in the HPLC system, and the length made as short as possible to limit band broadening. The HPLC and ICP-AES should be as close together, physically, as possible. The systems interface at the nebulizer.

For the carbohydrate project a Hildebrand Grid nebulizer (HGN) was used. See Figure 5. The sample solution is pumped into a circular groove where it flows across two platinum screens. High velocity argon is forced through a 0.17 mm opening in a sapphire crystal, blowing droplets of solution out of the screens forming a fine aerosol.<sup>5</sup> The amino acids project used a Teflon low-flow micro concentric nebulizer in lieu of the HGN because at a flow rate of 0.4 mL/min it



resulted in less noise and lower detection limits. See Figure 6. The attached dual concentric Scott-type spray chamber eliminates large particles, which are removed to waste by a peristaltic pump. The spray chamber modifies the aerosol so that only small, reproducible aerosol particles (1-5% of the sample) successfully flow into the horizontally positioned quartz torch. If the aerosol went directly from the nebulizer to the plasma, the signal would be very noisy due to variation in aerosol particle size.

Figure 4. HPLC-ICP-AES Schematic.

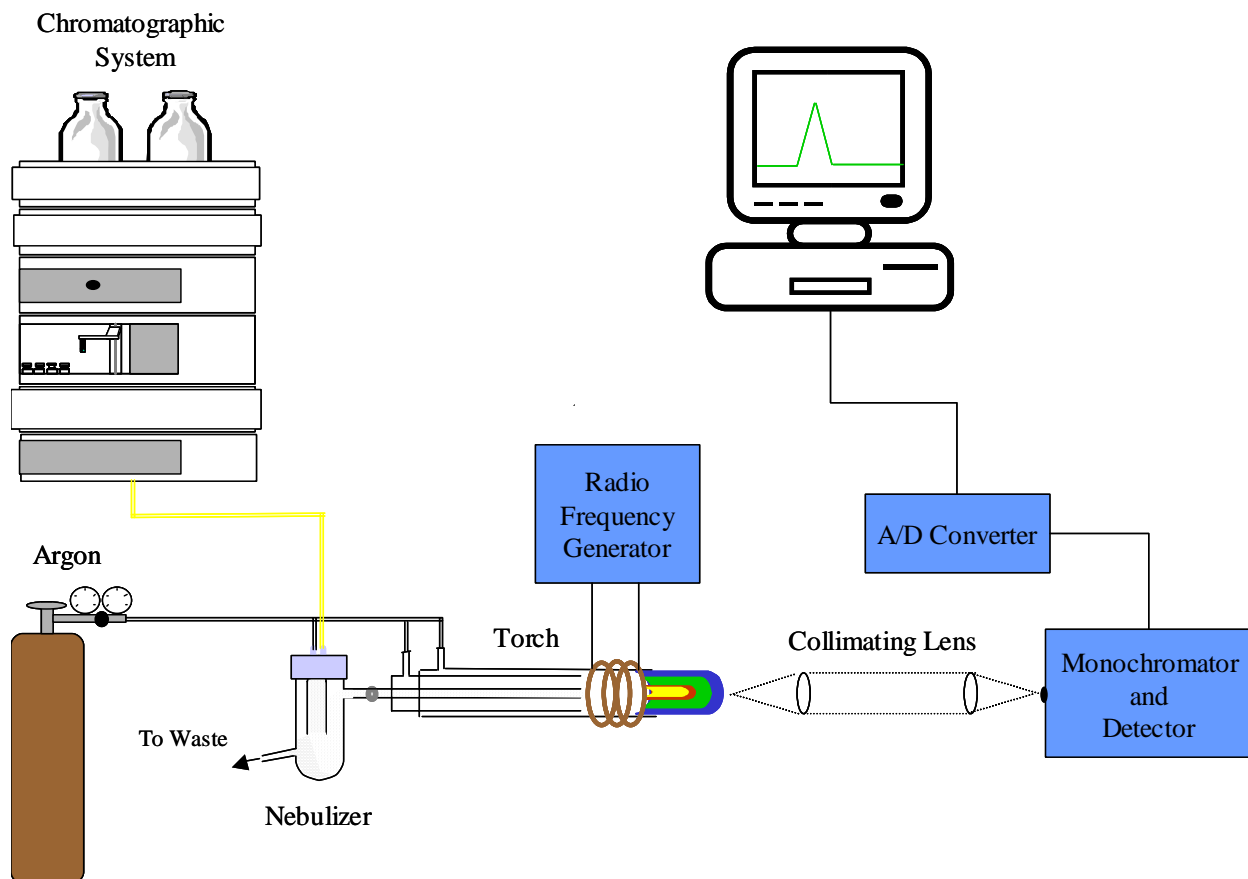


**Figure 5. Cross Sectional View of Hildebrand Grid Nebulizer.**

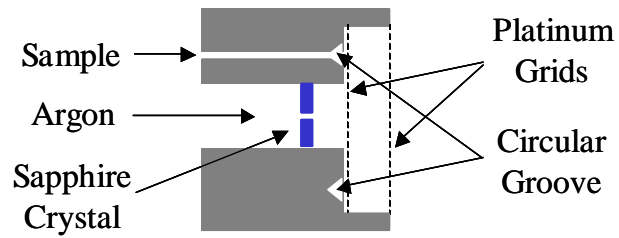
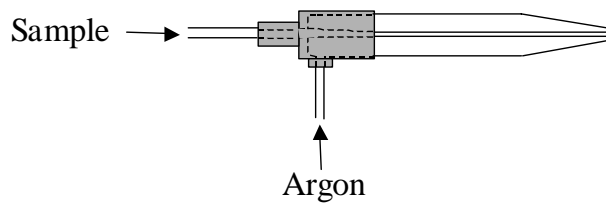


**Figure 6. Micro-Flow Concentric Nebulizer.**

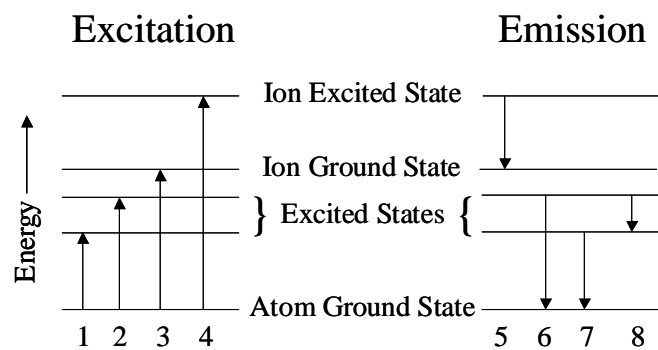


The torch consists of three concentric tubes. The aerosol flows through the innermost tube, called the injector tube. Argon flows between the injector tube and center tube, called the auxiliary flow, going directly under the plasma toroid to keep the plasma discharge away from the tubes. Also argon flows between the middle and outer tubes, called the plasma flow, moving in a spiral pattern to cool the center tube and center the plasma radially. The end of the torch is surrounded by a copper load coil that is cooled by deionized water circulating through the coil to a chiller unit.

A radio frequency generator, connected to the load coil, applies power to the coil resulting in an alternating current that oscillates back and forth in the coil at a rate corresponding to the frequency of the generator, 40.68 MHz. The generator is capable of operating at any power level up to a maximum of 2 KW.<sup>6</sup> A piezoelectric spark is applied to the plasma flow causing some argon atoms to lose electrons, which are then accelerated by the magnetic field resulting from the RF oscillation in the coil. This process is called inductive coupling. These electrons collide with other argon atoms in a chain reaction that results in a plasma of argon atoms, argon ions, and electrons sustained by the RF energy. Temperatures in the plasma range from 10,000 K at the base to 6,000 K at the apex. In the plasma the aerosol is desolvated, leaving dried sample particles, which are then vaporized into a gas. The gas molecules are then atomized. Further collisions with electrons and absorption from other emissions result in excitation and ionization. As the atom or ion decays, a photon is emitted. Each elemental atom or ion has characteristic radiation wavelengths. The intensity of the emitted light is directly proportional to

the number of atoms present. Excitation, ionization, and emission are diagrammed in Figure 7.

**Figure 7. Schematic of Excitation, Ionization, and Emission.** 1 and 2 are excitation to various excited states; 3 is ionization; 4 is excitation of an ion; 5 is ion emission; 6, 7, and 8 are atomic emission.



The plasma can be altered by changing any of four parameters. The generator power adds energy causing a more intense emission signal. The plasma flow and auxiliary flow determine radial and axial geometry of the plasma, respectively. **Increasing nebulizer pressure makes more small droplets that result in more analyte reaching the plasma, again causing a more intense emission signal.** This is limited though because too high of pressure will blow the droplets against the spray chamber wall where they will drain to waste. The delivery rate of the solution to the nebulizer also affects the intensity of the emission signal, but the rate is optimized to the HPLC separation rather than ICP-AES signal intensity.

The characteristic radiation from the plasma is collected by a monochromator, which sorts the radiation by wavelength. The radiation is then sent to a detector. However, the Leeman Labs software does not allow for continuous collection of data at a given wavelength for the duration of the separation, so the system optics are bypassed. The software is only used to maintain the plasma. An optics board is set-up adjacent to the instrument to allow for addition of lenses, monochromator, and detector that collect and send signal to an independent recording device. For these projects both a photomultiplier tube (PMT) and a charge-coupled device (CCD) are used.

### **HPLC-ICP SYSTEM CONSTRAINTS**

The principal resonance lines for nonmetals are in the vacuum ultraviolet region (10-200 nm). Less intense spectral lines in the visible region result in poor detection limits. Elements that emit in the vacuum-ultraviolet region have a limited number of detection methods available. Some organic compounds, such as

carbohydrates and amino acids, lack chromophores that result in absorption above 200 nm and do not natively fluoresce. Therefore the popular UV detector is generally not employed to analyze such samples. Chemical derivatization (e.g. fluorescence tagging) is performed either pre-column to enhance separation and improve detection or post-column solely to facilitate detection. Although frequently employed, derivatization reactions are often time-consuming and can add complexity to the determination procedure. Otherwise, a universal detector, such as refractive index, may be used to determine native, underivatized compounds. However, refractive index is vulnerable to minor mobile phase and environmental changes and is generally limited to major determinations because of its poor sensitivity.

Element-specific detection methods for high performance liquid chromatography (HPLC) include flame atomic absorption spectroscopy, inductively coupled plasma atomic emission spectroscopy (ICP-AES), and inductively coupled plasma-mass spectrometry (ICP-MS). ICP-AES offers simultaneous multi-element selective chromatographic detection at ultra trace levels with less interference effects than atomic absorption spectroscopy. Mass spectrometry was later introduced as a detection method for ICP. It separates based on mass to charge ratios ( $m/z$ ) and therefore can differentiate isotopes for speciation work. ICP-MS is, in general, more sensitive than ICP-AES and also more expensive.

ICP can be easily coupled to high performance liquid chromatography (HPLC) due to similar flow rates. ICP-AES takes advantage of unique elemental emission wavelengths. The spectra for dozens of elements can be detected simultaneously under a single set of excitation conditions. More expensive optical equipment with



high resolution is required to reduce or eliminate spectral interference from these highly complex spectra.

The viewing position of the emission from the plasma can be either axial (horizontal) or radial (vertical) with respect to the spectrometer system. Radiation from the center of the plasma viewed end-on (axial) results in improved detection limits by 4-10 times.<sup>7</sup> This is because axial viewing realizes a longer path that results in higher analyte signal. However, in this mode more matrix-induced interferences are seen and the tail of the plume, which is cooler, is in the optical path. In the cooler regions self-absorption occurs, resulting in a smaller linear dynamic range. These negative effects can be countered by employing a shear gas to push the tail up and out of the optical path. Lower limits of detection are achieved in the axial position.

HPLC-ICP can have poor detection limits. The sensitivity of a chromatographic sample is generally 10 times less than if the sample had been directly aspirated from a vial. ICP limits of detection for carbon and phosphorus are 75 and 30  $\mu\text{g/L}$ , respectively.<sup>8</sup> The chromatographic injector limits the sample size, and the column separates the components so that the sample is effectively diluted prior to reaching the nebulizer. Most nebulizers are less than 5% efficient, sending the bulk of solution to waste. Further more, the peak width limits the integration time, since a number of points must be collected to form a chromatogram. Selection of the column and mobile phase is dependent upon the compounds to be separated and is key to successful chromatography. The scientist must decide what mode of separation is best: size exclusion, partition (normal- or reversed-phase), adsorption, or ion-exchange. For ICP detection, the element being monitored must

not be present in the mobile phase, or the signal-to-background ratio will be diminished resulting in very poor detection limits.

Using plasma as an excitation source also adds constraints to experimental design. The plasma is difficult to maintain with greater than 20% organic in the aerosol. Organic solvents have a small mean aerosol drop size, high evaporation rate, and therefore a high transport rate. A lot of organic solvent cools the plasma, making it less stable or even extinguishing the plasma. Therefore, ICP-AES is not a suitable detector for all modes of liquid chromatography. An aqueous separation is ideal for ICP-AES detection, and limited organic can be used as long as carbon emission is not the line of interest. Oxygen absorbs radiation below 190 nm. Therefore when determining elements that emit at wavelengths below 190 nm, the spectrometer's optical path must be purged with nitrogen (or argon) and/or placed under a vacuum to reduce background noise and increase sensitivity. As an excitation source, argon plasma is only effective for elements with ionization energies less than argon.

### **CARBON DETERMINATION**

Some limitations must be taken into account with the HPLC-ICP system in order to use a carbon emission line for carbon determination. It is impossible to remove all carbon from the mobile phase, since it is so abundant on earth. Air contains carbon, which becomes entrained into the plasma, and significantly contributes to background. In order to monitor the carbon emission line, the mobile phase must be 100% aqueous, containing no organic solvent or buffer with any carbon. Therefore chromatography could be reversed-phase partition,

adsorption, ion-exchange, or exclusion by gel filtration. For reversed-phase chromatography, the column's stationary phase must not undergo phase collapse when exposed to 100% aqueous mobile phase for extended periods of time or else retention times will not be reproducible.

When using a multi-channel degasser and monitoring the carbon emission line, it is critical for all channels to be filled with non-organic mobile phase. Dissolved gas in the solvent permeates through the tubular plastic membrane into the vacuum, along with solvent vapors. These vapors can also permeate into the other channels' tubular plastic membranes. If organic solvent is present in any of the channels, the carbon content of the mobile phase will increase, thereby decreasing the signal-to-background ratio.

For amino acid determination a buffer is required to maintain reproducible separations. At different pH the elution order of some compounds change. The buffer should have  $pK_a$  at least plus or minus one pH unit from each analyte's  $pK_a$  to obtain a reproducible retention time. For carbon emission detection the buffer must not contain any carbon. A phosphate buffer at pH 7 is used for the amino acid project. A summary of research that used HPLC-ICP-AES to determine carbon is at Table I.

**Table I.** Carbon determination by HPLC-ICP-AES.

Sample	HPLC	Nebulizer	Wavelength	MDL	LOD for C	Ref.
Metalloproteins	Size exclusion	Cross flow	247.6	n.r.*	n.r.	9
Amino acids	Ion exchange	Cross flow	193.09	30-50 µg/mL	200 ng	10
Saccharides, Poly(ethylene glycol)	Size exclusion	Cross flow	247.9	n.r.	800 ng	11
Short alkyl chain alcohols	Ion exchange	Cross flow	247.86	n.r.	100-200 ng	12
Carmel colors	Size exclusion	n.r.	n.r.	n.r.	n.r.	13
Fruit juices	Ion exchange	Hildebrand grid	193.09	0.05 µg	n.r.	14

\* Not reported.

Reference 14 is the published report of the carbohydrate project and is located in Appendix A. The amino acid project is currently in review to be published in *Applied Spectroscopy* and is located in Appendix B.

## CONCLUSION

Through this research, ICP-AES is proven to be a sensitive, universal detector for HPLC and non-metal analysis. With improved stationary phase technology, an increasing number of compounds could be separated, making HPLC-ICP-AES the method of choice. This method eliminates derivatization and its associated contamination possibilities, eliminates the trade-off between multiple wavelength monitoring and sensitivity by monitoring selected atomic emission wavelengths, eliminates equilibration time between injections by using an isocratic separation, and allows for the use of a single calibration standard for all compounds or elimination of calibration curves altogether by the use of an internal standard. Although current systems are expensive, less expensive and lower powered ICP systems could be specifically designed for the exclusive purpose of non-metal emission detection. Detection limits could be improved by successful elimination of background signals, especially in carbon. The phospholipid project should mirror the results of the carbon emission studies, demonstrating the method's value in determining phosphorus-containing compounds.

- 
1. Reference Manual for HP 1100 Series Quaternary Pump, 2d Ed., Hewlett-Packard Company, 1996: Germany, pg 31-32.
  2. Reference Manual for HP 1100 Series Autosampler, 2d Ed., Hewlett-Packard Company, 1996: Germany, pg 34.
  3. Reference Manual for HP 1100 Series Thermostated Column Compartment, 2d Ed., Hewlett-Packard Company, 1996: Germany, pg 26.
  4. Reference Manual for HP 1100 Series Diode Array Detector, 2d Ed., Hewlett-Packard Company, 1996: Germany, pg 28.
  5. PS Series ICP/Echelle Spectrometer Manual, Rev 1.0, Leeman Labs, Inc, Hudson, NH, pg E-I 8.
  6. PS Series ICP/Echelle Spectrometer Manual, Rev 1.0, Leeman Labs, Inc, Hudson, NH, pg E-I 14.
  7. Skoog, D. A.; Holler, F. J.; Nieman, T. A. *Principles of Instrumental Analysis*, Harcourt Brace and Company, Philadelphia: 1998, 232.
  8. Manning, T. J.; Grow, W. R. *The Chemical Educator* **1997**, *2*, 1-19.
  9. Morita, M.; Uehiro, T.; Fuwa, K. *Anal. Chem.* **1980**, *52*, 351-352.
  10. Yoshida, K.; Hasegawa, T.; Haraguchi, H. *Anal. Chem.* **1983**, *55*, 2106-2108.
  11. Jinno, K.; Nakanishi, S.; Nagoshi, T. *Anal. Chem.* **1984**, *56*, 1977-1979.
  12. Jinno K.; Nakanishi, S.; Fujimoto, C. *Anal. Chem.* **1985**, *57*, 2229-2235.
  13. Maitani, T.; Kubota, H.; Yamada, T. *Food Additives and Contaminants* **1996**, *13*(8), 1001-1008.
  14. Peters, H. L.; Levine, K. E.; Jones, B. T. *Anal. Chem.* **2001**, *73*, 453-457.

**A Multi-Analyte Calibration Curve for High Performance Liquid  
Chromatography with an Inductively Coupled Plasma  
Carbon Emission Detector**

Heather L. Peters, Xiandeng Hou,<sup>†</sup> and Bradley T. Jones\*

Department of Chemistry, Wake Forest University, Winston-Salem, NC 27109, USA

e-mail: jonesbt@wfu.edu      fax: (336) 758-3889

---

<sup>†</sup> College of Chemistry, Sichuan University, Chengdu, Sichuan 610064, P.R. China

**ABSTRACT**

A liquid chromatography system with an inductively coupled plasma detector is used to prepare a single calibration curve that is useful for multiple analytes. The detector monitors the atomic emission from carbon at 193.09 nm. Hence the analytes need not exhibit appreciable molar absorptivity or native fluorescence. Since the carbon signal is independent of molecular structure, the sensitivities for different compounds are similar as long as nebulization efficiencies are comparable. In fact, with a suitable internal standard, no calibration curve is necessary. The capability of the system is demonstrated with a test mixture of nine amino acids separated with a C30 reversed phase column and a 20 mM phosphate buffered mobile phase. The system provides a detection limit of 30 ng carbon. A multi-analyte calibration curve is prepared with 135 distinct measurements: each of nine analytes, at five different concentrations, repeated in triplicate. The average relative standard deviation for 27 measurements of different amino acids at a given concentration is 2.5%. Clearly, a single analyte will suffice for the calibration of all nine test compounds. Similarly, the internal standard method provides an average percent error of 2.0% for the determination of 45 different amino acid concentrations using only a single replicate for each sample.

**INDEX HEADINGS:** inductively coupled plasma, high performance liquid chromatography, carbon emission, amino acids



## INTRODUCTION

The inductively coupled plasma (ICP) has been used sporadically as a carbon emission detector for high performance liquid chromatography (HPLC).<sup>1,2,3,4,5,6</sup> The motivation behind the marriage of these techniques is the continuing search for a universal detector for liquid chromatography. In gas chromatography, for example, the flame ionization detector (FID) provides a significant signal for any carbon containing compound. The FID, then, is nearly universal, effectively detecting just about any analyte of interest, with the notable exceptions of water and hydrogen peroxide. Unfortunately, in HPLC the analytes are carried in a flowing stream of solvent, rendering the use of the FID a challenge. To begin with, the HPLC mobile phase should not produce a background signal at the detector, so organic modifiers are a problem. Hence, most HPLC-FID systems employ totally aqueous mobile phases. Secondly, the flame in the FID is normally not capable of accepting large volumes of liquid, so many different coupling arrangements have been explored.

The use of GC detectors in HPLC was reviewed in 1991.<sup>7</sup> Prior to that time, most HPLC-FID couplings involved desolvation and/or mechanical introduction of the sample. Early on, a porous disk was employed for these purposes.<sup>8</sup> A moving wire was also used to convey the eluent from a microbore HPLC column to the FID.<sup>9,10</sup> Similarly, a quartz fiber moving belt was developed for eluent deposition, desolvation and transport to the FID.<sup>11,12,13</sup> More recent approaches have included the development of an aerosol alkali FID,<sup>14</sup> a thermospray FID,<sup>15</sup> a novel headspace cell,<sup>16</sup> a novel drop interface,<sup>17</sup> and an eluent-jet interface for microbore LC.<sup>18</sup>

Finally, HPLC has been coupled to the FID through an interface similar to those used in HPLC mass spectrometry.<sup>19,20</sup>

The ICP, on the other hand, has a conventional flow rate that is quite compatible with most HPLC separations. Coupling the two systems is therefore comparatively straight forward. An HPLC-ICP system is an expensive alternative however, and the use of organic mobile phase modifiers remains undesirable. Nevertheless, the robustness of the plasma, the simplicity of the interface, and the potential for simultaneous multi-element analyses has driven further development.

The literature describing systems used for the HPLC-ICP determination of carbon containing compounds is limited. Morita and coworkers developed a system for the analysis of metalloproteins.<sup>1</sup> They performed gel permeation chromatography with a 0.9% NaCl mobile phase. A conventional cross flow nebulizer was directly connected to the HPLC eluent (1.0 mL/min) to carry the analytes to the argon plasma. The atomic emission line for C (247.86 nm) was monitored simultaneously with those for P, Co, and several other elements. This system allowed for the calculation of the atom number ratio for a vitamin B<sub>12</sub> sample. The calculated ratio was C<sub>64.2</sub>P<sub>0.93</sub>Co<sub>1</sub>, compared to the theoretical value of C<sub>63</sub>PCo.

Three years later, Haraguchi's group monitored the C emission line at 193.09 nm for the HPLC-ICP determination of underivatized amino acids.<sup>2</sup> They employed a strong cation exchange resin as the stationary phase and pH adjusted aqueous solutions of NaH<sub>2</sub>PO<sub>4</sub> as the mobile phase. A 1.4 mL/min flow rate was employed and the HPLC eluent was transported directly to the ICP's cross flow nebulizer using a 300 mm length of 0.5 mm i.d. Teflon tubing. Eight amino acids were detected

with the system. The authors noted that carbon dioxide contamination had the potential to give rise to a significant background emission signal. The sources of contamination were identified as air leakage in the gas lines, the presence of CO<sub>2</sub> in the solutions, or simply atmospheric gas becoming entrained in the plasma flow. They also noted that the carbon emission line at 193.09 nm gave rise to a higher signal-to-background ratio than the 247.86 nm line. The system achieved a carbon detection limit of 200 ng (S/N=2) and a dynamic range of 3.5 orders of magnitude. Equally impressive was the fact that the relative intensities for each of the eight amino acids agreed within 3% error. Thus, a single calibration curve could be used to quantitatively determine all analytes.

Shortly thereafter, Jinno and coworkers developed a micro-HPLC-ICP system that monitored the carbon emission line at 247.86 nm.<sup>3</sup> The microcolumn was packed with SC-220 gel and the mobile phase was distilled water. The system employed a flow rate of 16 μL/min and the eluent was sent directly to a "no spray chamber" cross flow nebulizer via a stainless steel capillary. The system provided near baseline resolution for three saccharides: raffinose, glucose, and arabinose. The observed detection limit was 800 ng C (S/N=2). The same group later improved detection limits to 100-200 ng C by modifying the nebulization system.<sup>4</sup> In that work, various small organic compounds were detected (from chloroform to cyclohexane), and those with higher volatility tended to give higher carbon emission intensities.

More recently, Maitani and coworkers used a gel filtration column coupled to an ICP for the analysis of commercial caramel colors.<sup>5</sup> Their mobile phase was aqueous 10 mM phosphate buffer (pH 5.5) at a flow rate of 0.6 mL/min. The eluent

was introduced continuously to the nebulizer tube of the ICP. Four elements (C, S, Ca, and Fe) were monitored simultaneously. Carbon detection limits were not reported. The system was used to determine the molar ratios of C relative to S in the various coloring agents. Though unmentioned in the text, several chromatograms in the manuscript demonstrated an advantage of the C emission detector over the conventional uv-vis absorption detector. The absorption chromatograms were comprised of many large overlapping peaks, while the C emission chromatograms were clean. Peak intensities for the ICP system depended only upon the amount of C present, not on the relative molar absorptivity, so only those analytes present at the highest relative concentration dominate the chromatogram.

The axial viewing configuration was first employed in an HPLC-ICP C emission system in 2001.<sup>6</sup> In this case, a calcium form ligand exchange column was used in conjunction with a deionized water mobile phase for the separation of carbohydrates. The HPLC eluent flowing at 0.6 mL/min was coupled directly to the ICP via a one-meter segment of polyetheretherketone (PEEK) tubing connected to a Hildebrand grid nebulizer. The C emission line at 193.09 nm was employed. The carbon detection limit was 20 ng (S/N=3), or approximately 10 times lower than the previously reported detection limits for saccharides.<sup>3,4</sup> As reported in earlier works, the authors noted that a single calibration curve sufficed for multiple analytes, and the C emission detector provided a cleaner sample chromatogram (specifically for the determination of sugars in fruit juices).

The results reported below further characterize that system. The saccharide specific column is replaced with one with a more generic stationary phase. The C30

reversed phase column may be applied to a wide variety of practical separations. The column is compatible with a 100% aqueous mobile phase. A group of easily separated amino acids is used as a test mixture, as suggested by previous workers.<sup>2</sup> The goal of the investigation is to determine if a single calibration standard will indeed suffice for such a mixture, and if an internal standard technique might eliminate the need for a calibration curve altogether.

## EXPERIMENTAL

Figure 1 is a schematic diagram of the HPLC-ICP system.<sup>6</sup> An Agilent Technologies Series 1100 HPLC (Palo Alto, CA, USA) with vacuum degasser, quaternary pump, autosampler, thermostated column compartment, and photodiode array (PDA) detector separated the amino acids. A one-meter segment of 0.178 mm I.D. x 1.59 mm O.D. polyetheretherketone (PEEK) tubing interfaced the chromatographic components of this system to a Leeman Labs (Hudson, NH, USA) Direct Reading Echelle ICP-AES, which generated the plasma emission. The proximity of the two instruments to one another determined the minimum length.

Amino acids were purchased from Aldrich Chemical (Milwaukee, WI, USA). Phosphoric acid 85%, HPLC grade, was purchased from Fisher Scientific (Fair Lawn, NJ, USA). Deuterium oxide, 99.9 atom percent deuterium, which was used as the void marker, was purchased from Aldrich Chemical (Milwaukee, WI, USA). At the end of each day, 0.5 mM sodium azide (Sigma Chemicals, St. Louis, MO, USA) was flushed through the system and left in the column as an antibacterial agent.

The isocratic mobile phase used throughout this investigation was distilled and deionized water from a Millipore MILLI-Q system (Bedford, MA, USA) with a resistivity of 18 M $\Omega$ /cm. A 20 mM phosphate buffer, adjusted to pH 7 with sodium hydroxide, was added. The mobile phase was filtered (0.45  $\mu$ m) before pouring into the HPLC solvent dispensing bottles. Mobile phase was placed in all four channels to eliminate the potential for carbon contamination from organic solvents in the vacuum degasser.

Each of the amino acids was dissolved separately into the mobile phase and injected onto the column to determine retention times. A mixture of nine that provided near baseline resolution was selected as a test mixture, and a stock solution was prepared. Calibration standards were prepared from serial dilutions of the stock solution.

Sample aliquots of 20  $\mu$ L were injected by the autosampler onto a 250 mm x 4.6 mm Develosil<sup>®</sup> 5 $\mu$  RP-Aqueous C30 column (Nomura Chemical, Seto, Japan). A 10 mm x 4 mm Develosil<sup>®</sup> RP-Aqueous guard column preceded the analytical column and was connected by a 3 cm length of 0.178 mm I.D PEEK tubing. The column compartment was maintained at 25<sup>°</sup>C for optimal separations. The C30 stationary phase was selected as a general column that could be applied to a multitude of separations using a 100% aqueous mobile phase. The column was not chosen to optimize the amino acid separation, which might be better performed with an ion exchange resin.

Column eluent was introduced through a nebulizer with industrial grade argon at 45 psi. The nebulizer was a perfluoroalkoxy grade Teflon<sup>®</sup> concentric MicroFlow nebulizer for AES (CPI International, Santa Rosa, CA, USA). The MicroFlow nebulizer can be used at flow rates up to 2 mL/min. The Scott-type spray chamber eliminated large particles from the resulting aerosol, which were evacuated by a peristaltic pump. Small, reproducible aerosol particles that successfully navigated the spray chamber flowed into the horizontally positioned plasma generated by 1.2 KW.

The carbon emission signal emanating from the ICP was collected by a fused silica lens (25 mm diameter, 150 mm focal length) placed 150 mm from the plasma.

This lens directed a collimated beam to a similar lens located 150 mm from the detector, producing a 1:1 image of the plasma on the entrance slit of a 0.35 m scanning monochromator (McPherson Model 270, Acton, MA, USA) with a photomultiplier tube (PMT) detector. The monochromator employed a 1200 gr/mm grating, providing a reciprocal linear dispersion of 2 nm/mm. The entrance and exit slits were set at a width of 30  $\mu\text{m}$ , providing a spectral bandpass of 0.06 nm at the carbon emission wavelength (193.09 nm). A personal computer equipped with an A/D converter collected and stored the chromatogram. A data point was collected every 500 milliseconds, and four successive points were averaged dynamically. For comparison purposes, chromatograms were also obtained using the standard uv-visible absorption detector provided with the HPLC.

## RESULTS AND DISCUSSION

Figure 2 shows amino acid chromatograms recorded at a flow rate of 0.4 mL/min at 25°C and pH 7. The sample solution injected contained equal concentrations of carbon for each amino acid. Hence the peaks for the ICP-AES detector should have equivalent areas, while those for the uv-visible detector, which depend upon the molar absorptivity of the amino acid, vary greatly. The efficiency of the separation, expressed as the number of theoretical plates (N) for the leucine peak, was 14,000. Analytical figures of merit for the method are reported in Table I.



The baseline fluctuations observed for the carbon emission detector arise from the noise associated with background emission from the ICP. This background signal arises from two sources: carbon contamination in the plasma, and broadband continuum emission from the plasma. The magnitude of the background signals may be corrected by subtraction, but the associated noise will appear as a fluctuation in the baseline (Figure 2b). A monochromator/PMT combination with a higher resolution would reduce the noise arising from the continuum emission, but the carbon contamination is difficult to address, and hence limits the detection power of the technique.

The carbon emission detector is not adversely affected by compounds with large molar absorptivity. The peak for valine in Figure 2a for example appears as a small shoulder on the large histidine peak. In fact, the histidine peak is well above the linear range in Figure 2a, even though it is present at approximately the same concentration as valine. In Figure 2b, the peaks are baseline resolved. If the amino acids were in a complicated sample matrix, other species present at low concentration, but exhibiting unusually high molar absorptivity, might behave in a similar manner. The species with the highest carbon concentration in the sample, no matter what they are, will give rise to the largest signals at the carbon emission detector. For histidine and methionine the linear dynamic range was exceeded for uv-visible detection at approximately 2 mg/mL.

A five-point calibration curve was prepared spanning the range 200 to 1000  $\mu\text{g/mL}$  carbon (approximately 400 to 2000  $\mu\text{g/mL}$  amino acid). The sensitivity, or slope of the calibration curve, should be identical for each amino acid since the signal depends only upon carbon. In this case a single calibration curve should

suffice for all of the separated amino acids. In Figure 3 for example, each data point represent the mean of three replicates for each of the nine amino acids at the given concentration ( $n=27$ ). The error bars represent the standard deviation in those 27 measurements. The extremely tight fit demonstrates that a single calibration curve is sufficient, and any of the amino acids could be used as the lone standard. The detection limits for the amino acids are listed in Table I. A detection limit of  $3 \mu\text{g/mL}$  amino acid corresponds to a carbon detection limit of  $1.5 \mu\text{g/mL C}$ , or an absolute C detection limit of  $30 \text{ ng carbon}$  ( $S/N=3$ ). Furthermore, if a calibration curve is prepared as carbon concentration versus emission signal, then that curve can work for all compounds (even non amino acids), so long as they have similar nebulization efficiencies in the ICP. Then if the identity of the compound is known, one can calculate its concentration based upon its mass percent carbon. Such a technique would be an efficient, time-saving device that reduces preparation and instrument run time for calibration standards to one universal set.

Another option is to use a carbon containing internal standard. Norleucine was selected for this purpose because it is similar to the compounds being determined, it does not occur naturally in proteins, and its retention time ( $18.7 \text{ min}$ ) is distinct from other amino acids in the test set. A compound with an unknown concentration could be determined by simply spiking the sample with a known amount of norleucine. The peak area for the analyte could then be compared to the peak area of the norleucine to find the carbon concentration of the analyte. Since carbon sensitivity is independent of amino acid structure, no calibration curve is needed (i.e. the analyte has the same carbon emission

sensitivity as the internal standard). Once the carbon concentration of the analyte is known, the analyte concentration is determined simply by dividing by the mass percent carbon in the amino acid.

To evaluate the procedure, ten test mixtures were prepared. Each test mixture contained 1100  $\mu\text{g/mL}$  of norleucine (600  $\mu\text{g/mL}$  carbon). In addition, each mixture also contained either four or five additional amino acids at varying concentrations. Each amino acid appeared in five test mixtures, so a total of 45 different "known" concentrations were determined by the technique. Each mixture was analyzed a single time. The results are shown in Figure 4. The units for each axis are  $\mu\text{g/mL}$  amino acid, so the results have been converted from raw carbon concentration. The trend line on the plot has a slope of one and an intercept of zero. The average percent error for the 45 measurements is 2.0%. These results are striking, considering that no calibration curve was employed and the nine compounds had different retention characteristics. One might expect the precision to improve if multiple injections of the same analyte were performed at a given concentration, as with the calibration curve in Figure 5. This technique, of course, requires that the analyte's identity be known. Otherwise, only approximate analyte concentration can be inferred from exact carbon concentration.

Recovery studies were conducted for the amino acids using standard solutions near the upper end of the calibration curve (either 700 or 800  $\mu\text{g/mL}$  C). Three replicate measurements were obtained for each compound. The average percent recovery was 100.9% with a standard deviation of 3.1% (using the calibration curve method). Recovery results for each amino acid are also included in Table I.

## CONCLUSION

There is not yet a simple method for the determination of underivatized amino acids that achieves the sensitivity of fluorescence detection. However, with improved stationary phase technology, HPLC-ICP-AES could become the method of choice. This method eliminates derivatization and its associated contamination possibilities, eliminates the trade-off between multiple wavelength monitoring and sensitivity by monitoring the carbon emission wavelength, eliminates equilibration time between injections by using an isocratic separation, and allows for the use of a single calibration standard for all compounds or elimination of calibration curves altogether by the use of an internal standard. A commercially available ICP-AES instrument can be used as a sensitive, universal detector for carbon in amino acids following a reversed phase HPLC separation procedure. Although current systems are expensive, less expensive and lower powered ICP systems could be specifically designed for the exclusive purpose of carbon emission detection. Detection limits could be improved by successful elimination of background carbon signals.

**Table I.** Analytical Figures of Merit for HPLC-ICP with Carbon Emission Detection at a Flow Rate of 0.4 mL/min.

	Mass Percent Carbon	Retention Time (min)	Detection Limit ( $\mu\text{g/mL}$ )	Percent Recovery
Lysine	49.2	6.7	5	100.6
Threonine	40.3	7.2	3	101.5
Arginine	41.2	7.6	3	100.2
Proline	52.2	8.5	3	107.5
Histidine	46.4	9.2	5	101.4
Valine	51.3	9.8	3	101.3
Methionine	40.3	13.8	5	99.3
Isoleucine	54.9	16.9	3	99.3
Leucine	54.9	17.6	2	100.6

**Figure 1.** Schematic Diagram of the HPLC-ICP system.

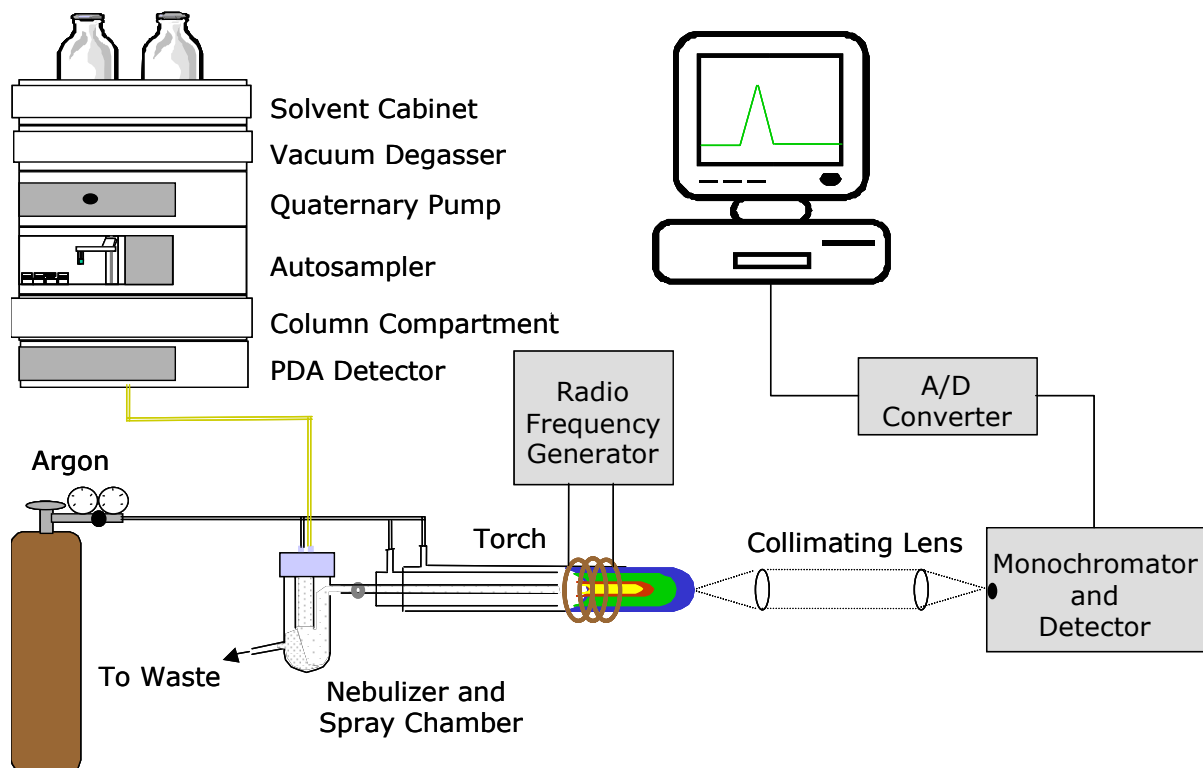
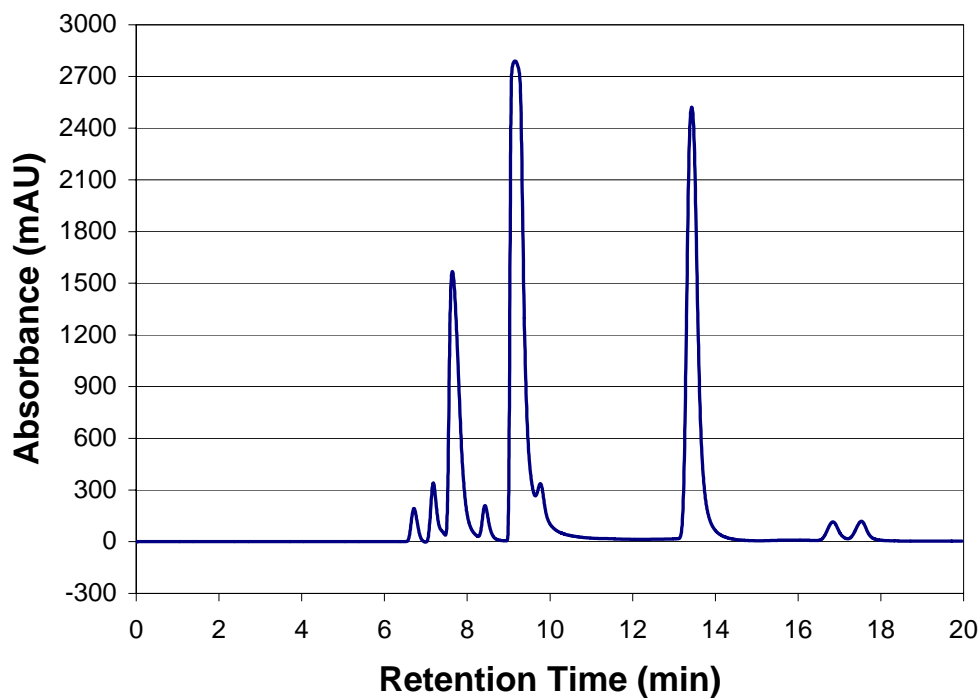


**Figure 2.** Chromatograms obtained from a single injection of a solution containing an equal amount of carbon ( $20\ \mu\text{g}$ ) from each of nine amino acids using a flow rate of  $0.4\ \text{mL}/\text{min}$ . L to R: lysine, threonine, arginine, proline, histidine, valine, methionine, isoleucine, and leucine.

a) UV-visible absorption at  $206\ \text{nm}$ .



b) ICP carbon emission at  $193.09\ \text{nm}$ .

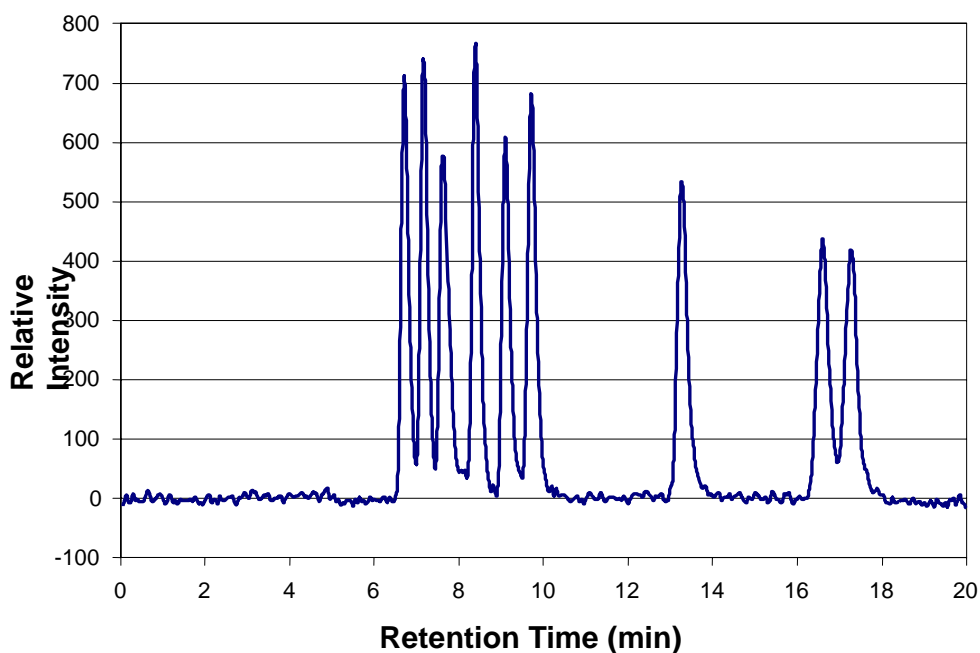


**Figure 3.** Single calibration curve constructed from data collected from nine different amino acids. Each data point represents the average signal for each of the nine compounds. Each measurement was performed in triplicate, so  $n=27$ . The error bars represent one standard deviation in the 27 measurements.

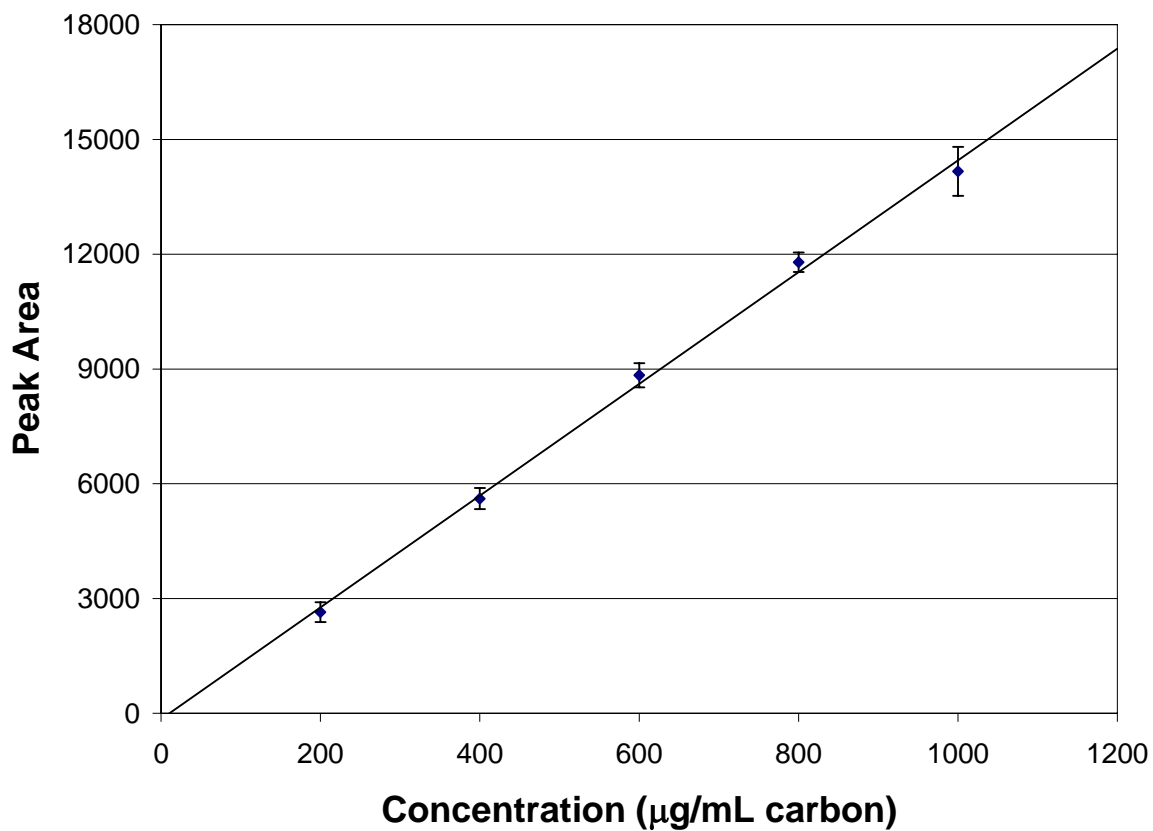
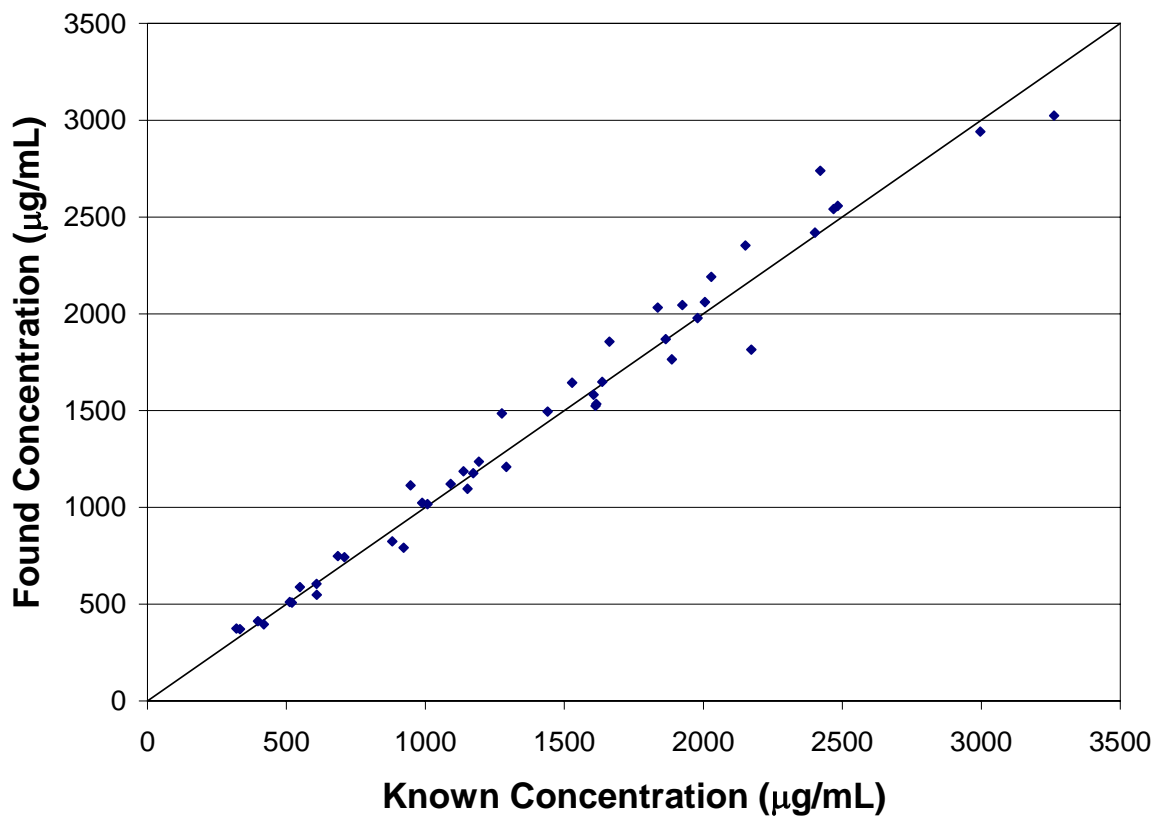




**Figure 4.** Accuracy of the internal standard method. Each data point represents a single measurement of the concentration of amino acid found using norleucine as an internal standard. No calibration curve was employed. Each of nine amino acids were determined at 5 different concentrations. On the trend line the amount found is the same as the known amount.



**REFERENCES**

---

1. M. Morita, T. Uehiro and K. Fuwa *Anal. Chem.* **52**, 351 (1980).
2. K. Yoshida, T. Hasegawa and H. Haraguchi, *Anal. Chem.* **55**, 2106 (1983).
3. K. Jinno, S. Nakanishi and T. Nagoshi, *Anal. Chem.* **56**, 1977 (1984).
4. K. Jinno, S. Nakanishi and C. Fujimoto, *Anal. Chem.* **57**, 2229 (1985).
5. T. Maitani, H. Kubota and T. Yamada, *Food Additives and Contaminants* **13**, 1001 (1996).
6. H.L. Peters, K.E. Levine and B.T. Jones, *Anal. Chem.* **73**, 453 (2001).
7. C.E. Kientz, G.J. Dejong and U.A.T. Brinkman, *J. Chromatogr.* **550**, 461 (1991).
8. J.J. Szakasits and R.E. Robinson, *Anal. Chem.* **46**, 1648 (1974).
9. H. Veening, P.P.H. Tock, J.C. Fraak and H. Poppe, *J. Chromatogr.* **352**, 345 (1986).
10. T. Tsuda, A. Nago, G. Nakagawa and M. Maseki, *J. High Res. Chromatogr.* **6**, 694 (1983).
11. J.B. Dixon, *Chimia* **38**, 82 (1984).
12. C.D. Pearson and S.G. Gharfeh, *J. Chromatogr.* **329**, 142 (1985).
13. C.D. Pearson and S.G. Gharfeh, *Anal. Chem.* **58**, 307 (1986).
14. E.D. Conte and E.F. Barry, *Microchem. J.* **48**, 365 (1993).
15. F.O. Disanzo, S.P. Herron, B. Chawla and D. Holloway, *Anal. Chem.* **65**, 3359 (1993).
16. C.A. Bruckner, S.T. Ecker and R.E. Synovec, *Anal. Chem.* **69**, 3465 (1997).
17. W.W.C. Quigley, S.T. Ecker, P.G. Vahey and R.E. Synovec, *Talanta* **50**, 569 (1999).
18. E.W.J. Hooijschuur, C.E. Kientz and U.A.T. Brinkman, *J. High Res. Chromatogr.* **23**, 309 (2000).
19. W.E. Neff, G.R. List and W.C. Byrdwell, *J. Chromatogr. A* **912**, 187 (2001).
20. W.C. Byrdwell, W.E. Neff and G.R. List, *J. Agr. Food Chem.* **49**, 446 (2001).

